Behaviour of soilbags subjected to monotonic and cyclic vertical loading

S. H. Liu[1], B. X. Fang[2], Y. Lu[3] and S. Chen[4]

[1]*Professor, College of Water Conservancy and Hydropower Engineering, Hohai University, Nanjing 210098, China*
[2]*PhD Candidate, College ofWater Conservancy and Hydropower Engineering, Hohai University, Nanjing 210098, China, E-mail: bxfang@hhu.edu.cn (corresponding author)*
[3]*Associate Professor, College of Water Conservancy and Hydropower Engineering, Hohai University, Nanjing 210098, China*
[4]*Postgraduate Student, China Water Resources Bei Fang Investigation, Design and Research Co. Ltd, Tianjin 300222, China*

Received 12 September 2021, accepted 07 December 2021

ABSTRACT: Soilbags have been successfully used in the reinforcement of building foundations that can function as the base isolation. A series of unconfined compression tests under monotonic and cyclic loading were conducted to investigate the static bearing capacity and the dynamic deformation behaviour of stacked soilbags. The results of monotonic loading tests demonstrate that the ultimate compressive strength and the tangent compression modulus of soilbags tend to relatively stable values of around 0.7 MPa and 6.73 MPa, respectively, when the number of layers exceeds three. Under cyclic loading, the accumulated vertical strain of stacked soilbags increases nonlinearly under the application of cyclic loading, reducing with each loading cycle and even reaching a relatively stable state where the vertical strain is primarily elastic, which can be described with an empirical formula with respect to the static vertical stress, the cyclic load ratio and the number of loading cycles. The resilient moduli of stacked soilbags change slightly during cyclic loading period, and increase with the increasing static vertical stress and the decreasing cyclic load ratio. The outcomes of this study demonstrate the feasibility of soilbags as the base isolation as they have prominent bearing capacity and stable deformation behaviour under cyclic loading.

KEYWORDS: Geosynthetics, soilbags, unconfined compression test, cyclic loading, bearing capacity, deformation, resilient modulus

REFERENCE: Liu, S. H., Fang, B. X., Lu, Y. and Chen, S. (2022). Behaviour of soilbags subjected to monotonic and cyclic vertical loading. *Geosynthetics International*. [https://doi.org/10.1680/jgein.21.00075]

1. INTRODUCTION

Earthquake is an unpredictable catastrophe, which might result in huge casualties and loss of properties including collapse of buildings, especially low-rise or middle-rise buildings. Over the past few decades, earthquake resistant measures have been mostly focused on increasing the strength and the stiffness of building structures to withstand the earthquake-generated inertial forces. Though these strengthening methods could safeguard building structures from collapse, some inevitable problems still exist, including damage to interior equipment and facilities. To effectively solve this problem, some base isolation methods have been consequently proposed to dissipate earthquake energy and minimize the intensity of earthquake vibrations before being transmitted into the superstructures. By means of these base isolators, displacements and accelerations of superstructures are greatly reduced consequently achieving the protection effect on building structures (Tsang 2008; Ahmad *et al*. 2009; Nanda *et al*. 2012). In recent years, some typical base isolation systems, such as rubber bearings (Kelly 1993), lead rubber bearings (LRB) (Robinson 1982) and friction pendulum bearings (FPB) (Mosqueda *et al*. 2004; Fenz and Constantinou 2006), have been successfully used in practical civil engineering. However, these proposed base isolation systems are generally used in high-rise buildings, which are easily neglected especially in low-rise or middle-rise buildings in rural areas owing to the high cost and complicated process of installation and maintenance. In recent years, some practical technologies to enhance seismic resistance for low-rise or middle-rise buildings, such as sand cushions, high-performance ferro-cement laminate

Offprint provided courtesy of www.icevirtuallibrary.com
Author copy for personal use, not for distribution

(HPFL) (Yao *et al.* 2014), and so on, have been proposed. Liu *et al.* proposed a new base isolation technology using soilbags (Liu *et al.* 2010) with advantages of good damping effect, low cost and convenient construction, which is suitable for most new buildings in rural areas.

Soilbags, namely geotextile bags filled with soils, gravels as well as other granular materials, have been commonly used in temporary structures such as flood prevention and diversion closure. As the result of numerous practices and the research pioneered by Matsuoka and Liu (1999, 2003), many advantages of soilbags, such as easy construction, low cost, high strength and wide availability of infilled materials, and so on have been revealed. Today, soilbags are increasingly used in the fields of civil, hydraulic and transportation engineering, for example the foundation reinforcement of buildings, subgrade treatment, construction of retaining walls as well as slope reinforcement. In recent years, a series of studies on soilbags have been carried out by Liu (2007), Liu and Matsuoka (2017), Liu *et al.* (2014, 2015, 2020, 2021), including the static and dynamic behaviours of soilbags, the frost heave prevention, improvement of bearing capacity for soft foundations, the treatment of expansive soil channel slope with soilbags, properties and construction of retaining walls with soilbags. There are also many studies on soilbags by other researchers, such as experimental studies on compressive strength and shear strength (Yamamoto *et al.* 2003; Lohani *et al.* 2006) as well as the numerical investigation of the mechanical properties and the reinforcement mechanism of soilbags (Tantono and Bauer 2008; Ansari *et al.* 2011; Cheng *et al.* 2016; Wang *et al.* 2019). The experimental and numerical research results illustrate that soilbags, with a damping ratio higher than 0.3 and variable horizontal stiffness under different vertical stresses and shear strains, have a great advantage in terms of vibration reduction and energy dissipation, which indicate that soilbags may be used for the base isolation materials. Field experiments on sandbag isolators installed beneath a full-scale building near an existing subway line performed by Sheng *et al.* (2020) indicated that the damping ratio of the sandbag isolator is high enough to resist resonant amplitudes and the subway-induced vertical vibration inside the building is effectively suppressed.

As a base isolation material for low-rise and middle-rise buildings, it is required to have sufficient bearing capacity and small dynamic deformation under vertical seismic loadings. In this study, a series of laboratory unconfined compression tests under monotonic and cyclic loadings were carried out on stacked soilbags to investigate their bearing and dynamic deformation properties. The evolutions of vertical stress-strain relation curve and tangent compression modulus of soilbags were discussed based on the results of monotonic loading tests. The accumulated vertical strain and resilient modulus of stacked soilbags under cyclic loading at different vertical stresses and cyclic load ratios were investigated.

2. TEST PROFILES

2.1. Testing apparatus

Figure 1 shows the testing apparatus used in this study. It includes a loading system and a data acquisition. The loading system consists of a counterforce frame, a hydraulic actuator and a square loading plate as well as a servo controlling unit. The square loading plate is connected to a quadrilateral truss structure to prevent its incline under the vertical loading. The hydraulic actuator can produce monotonic or cyclic vertical loads depending on the intensity of the input compressed oil. The servo controlling unit regulates the magnitude of monotonic or cyclic vertical loads and the number of loading cycles.

The data acquisition system can read and record the vertical load and displacement automatically. The vertical load applied on the soilbag sample was measured by using a load cell with a precision of ±0.01% full range (1000 kN), which was installed on the bottom of the hydraulic actuator. The vertical displacement of the soilbag sample was measured by using two displacement transducers with the precision of 0.0005 mm, which were diagonally set on the square loading plate. To ensure an accurate reading, all of the devices, especially the displacement transducers, were calibrated prior to each test.

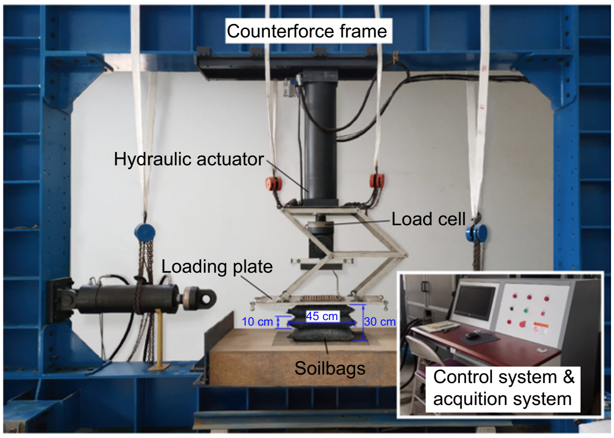

Figure 1. Schematic diagram of the test apparatus

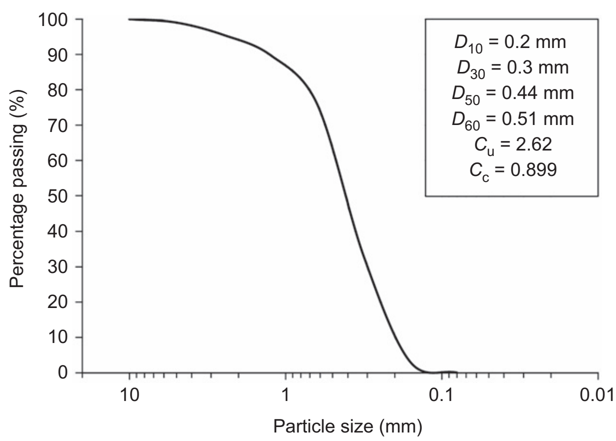

Figure 2. Particle size distribution curve of the sand filled in soilbags

Offprint provided courtesy of www.icevirtuallibrary.com
Author copy for personal use, not for distribution

Table 1. Scheme of unconfined compression tests for stacked soilbags

Test series	Load pattern	Static vertical stress σ_z^s (kPa)	Cyclic load ratio R_c	Soilbag layers L	Purpose of tests
A	Monotonic	—	—	1, 2, 3, 4, 5, 6	To study the bearing capacity of stacked soilbags with different layers under monotonic loading
B	Cyclic	100, 150, 200, 250	0.05, 0.15, 0.3, 0.4, 0.5	3	To study the dynamic deformation behaviour of stacked soilbags under cyclic loading

2.2. Sample preparation

Several soilbags were vertically stacked to form the test samples. The material filled in bags is a river sand with the grain size distribution as shown in Figure 2 and a specific gravity $G_s = 2.54$. It has a mean grain size of 0.44 mm, the coefficient of curvature $C_c = 0.899$ and the coefficient of uniformity $C_u = 2.62$. The moisture content of the river sand is 4.2%. The river sand has been proved to have a high damping ratio, especially in a relatively low stress condition (Yamamoto *et al*. 2003; Liu *et al*. 2014).

Black woven bags with the size of 60 cm × 50 cm, made of polypropylene (PP), were used in this research. The properties of these PP bags are as follows: the mass per square meter is 100 g; the warp and the weft tensile strengths are 17.18 kN/m and 22.72 kN/m, respectively; the warp and the weft allowable elongation are 18% and 24%, respectively. Approximately 30 kg sand was filled into one bag and the bag mouth was sealed using a portable sewing machine. After compaction, each soilbag has a dimension of approximately 45 cm long, 45 cm wide and 10 cm high.

2.3. Testing program

As materials for the base isolation layer, soilbags should provide a sufficient bearing capacity for superstructure and have small permanent deformation under dynamic loading. A certain spacing interval is reserved between the adjacent soilbags in the construction process to guarantee the seismic isolation effect through sufficient deformation of soilbags. In order to reflect the real stress condition of soilbags as base isolation layer, some unconfined compression tests, as listed in Table 1, were consequently planned and carried out in this research to investigate the bearing capacity and permanent deformation of soilbags. These tests have the following two loading schemes:

(1) Monotonic loading test

The monotonic unconfined compression tests were conducted on stacked soilbags with different layers to analyse the ultimate bearing capacity. Considering the possibility and appropriate thickness of base isolation layers in practice, the number of stacked layers L were chosen to be 1, 2, 3, 4, 5 and 6. For each sample of stacked soilbags, compressive load was raised monotonically at a rate of 0.5 kN/s until the sample was obviously damaged. Each test was repeated carefully at least twice. The acquisition frequency throughout the monotonic loading was 2 Hz.

(2) Cyclic loading test

To minimize the boundary influence of the top and the bottom rigid steel loading plates and consider the feasible thickness of foundation isolation layer in actual construction, the cyclic loading tests were performed on three-layered stacked soilbags. The pattern of cyclic loading comprised (*cf.* Figure 3):

(*a*) Load being raised monotonically at a rate of 0.5 kN/s to a given static load P_{stat}.

(*b*) Load maintained constant at this value until no further vertical deformation occurs or its increasing rate becomes negligible.

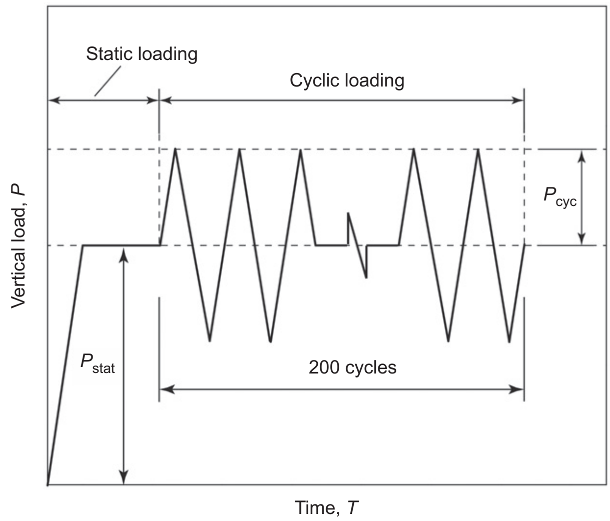

Figure 3. Schematic diagram of cyclic loading pattern

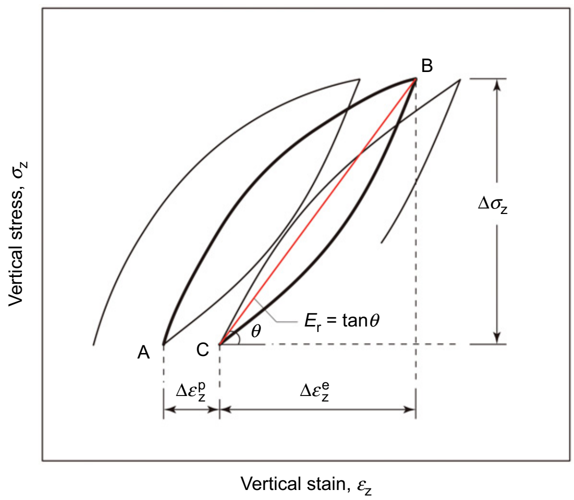

Figure 4. Schematic diagram of hysteresis loops

Offprint provided courtesy of www.icevirtuallibrary.com
Author copy for personal use, not for distribution

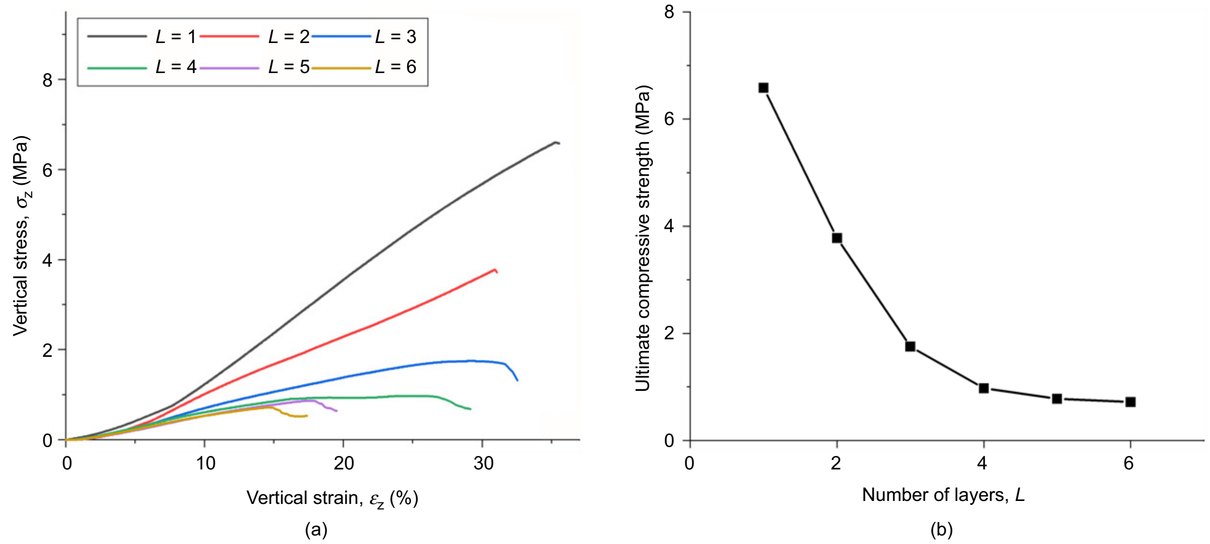

Figure 5. Results of monotonic loading tests on stacked soilbags with different layers: (a) $\sigma_z \sim \varepsilon_z$; (b) ultimate compressive strength ~L

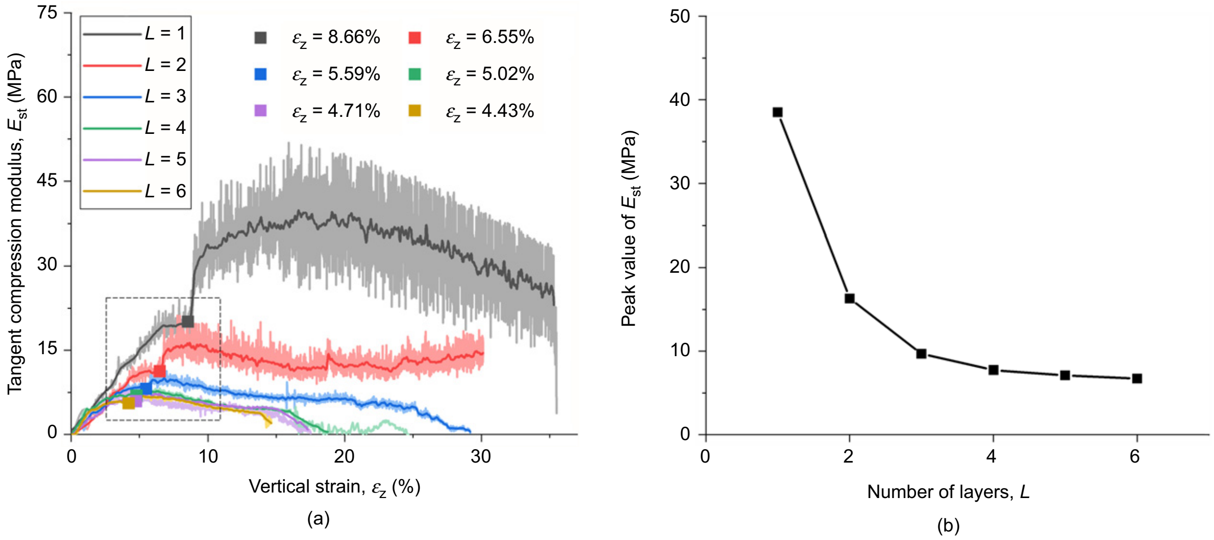

Figure 6. Tangent compression modulus of stacked soilbags with different layers: (a) $E_{st} \sim \varepsilon_z$; (b) peak value of $E_{st} \sim L$

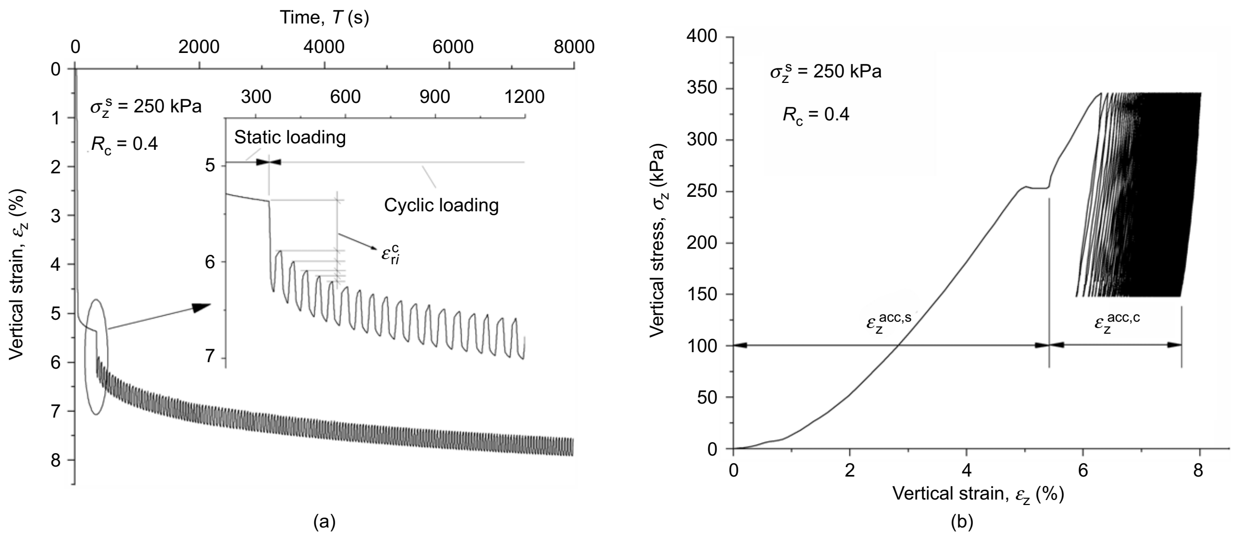

Figure 7. Compression curve of stacked soilbags under cyclic loading (σ_z^s = 250 kPa, R_c = 0.4): (a) vertical strain against time; (b) vertical stress against vertical strain

Offprint provided courtesy of www.icevirtuallibrary.com
Author copy for personal use, not for distribution

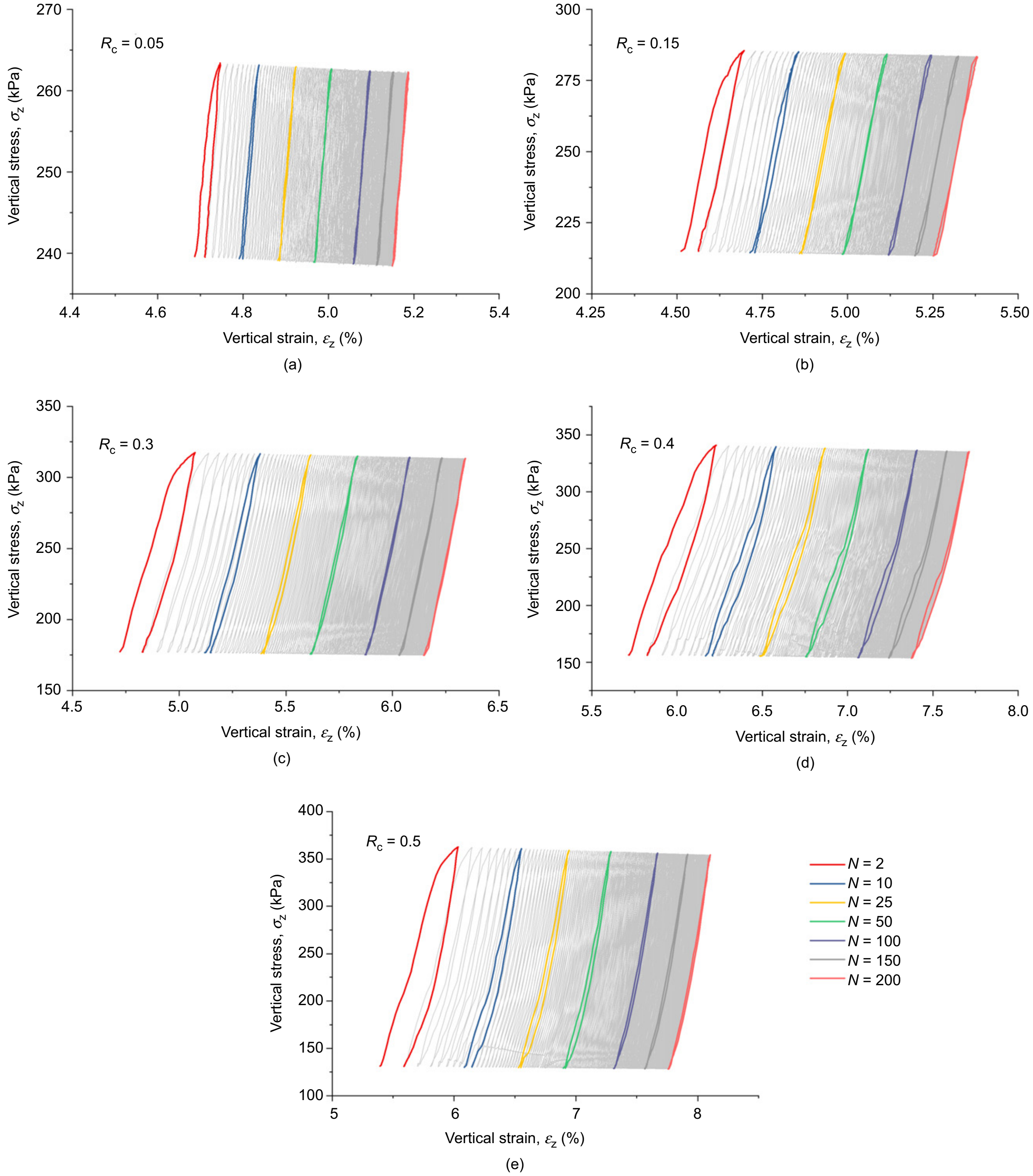

Figure 8. Hysteresis loops of stacked soilbags under cyclic loading for different cyclic load ratios at $\sigma_z^s = 250$ kPa: (a) $R_c = 0.05$; (b) $R_c = 0.15$; (c) $R_c = 0.3$; (d) $R_c = 0.4$; (e) $R_c = 0.5$

(*c*) Load then cycled by an additional amount P_{cyc}. The magnitude of the cyclic load P_{cyc} was related to the static load P_{stat} through the cyclic load ratio R_c ($= P_{cyc}/P_{stat}$) and was applied on the sample at a loading rate of 5.0 kN/s. The test stopped after 200 cycles.

As the characteristic value of foundation pressure of low-rise or middle-rise buildings is generally less than 300 kPa (MOHURD 2011), the static load P_{stat} was consequently selected to be 20 kN, 30 kN, 40 kN and 50 kN, with the corresponding static stress applied on the stacked soilbags of 100 kPa, 150 kPa, 200 kPa and 250 kPa, respectively. The cyclic load ratio R_c was selected to be 0.05, 0.15, 0.3, 0.4 and 0.5 to simulate different seismic fortification intensities.

2.4. Data processing

During monotonic or cyclic loading periods, the applied vertical load P and the corresponding vertical displacement δ were measured and recorded at every interval of

Offprint provided courtesy of www.icevirtuallibrary.com
Author copy for personal use, not for distribution

0.5 s. From the measurement, the vertical stress σ_z, the vertical strain ε_z and the tangent compression modulus E_{st} of the sample can be obtained. Considering the changes of the area and the height of the sample under vertical load, σ_z and ε_z are calculated as:

$$\sigma_z = \frac{P}{A_0}\left(1 - \frac{\delta}{h_0}\right) \tag{1}$$

$$\varepsilon_z = \ln\left(1 - \frac{\delta}{h_0}\right) \tag{2}$$

in which A_0 and h_0 are the initial area and height of the stacked soilbags, respectively.

For the monotonic loading, the tangent compression modulus E_{st} is calculated as the ratio of the vertical stress increment $\Delta\sigma_z$ to the vertical strain increment $\Delta\varepsilon_z$ at each data recording interval (0.5 s). For the cyclic loading, the resilient modulus E_r of the sample in one loading cycle is analysed, which is calculated as the secant slope of the hysteresis loop (Figure 4):

$$E_r = \frac{\Delta\sigma_z}{\Delta\varepsilon_z^e} \tag{3}$$

in which $\Delta\sigma_z$ and $\Delta\varepsilon_z^e$ are the increments of the applied vertical stress and the generated recoverable (elastic) vertical strain in one loading cycle, respectively. In Figure 4, $\Delta\varepsilon_z^p$ is the unrecoverable (plastic) vertical strain in one loading cycle, and θ is the inclination angle measured by connecting the two endpoints of the unloading curve in one loading cycle.

3. RESULTS AND DISCUSSION

3.1. Bearing behaviour of stacked soilbags

Figure 5a presents the evolution of the vertical stress with the vertical strain of stacked soilbags with different

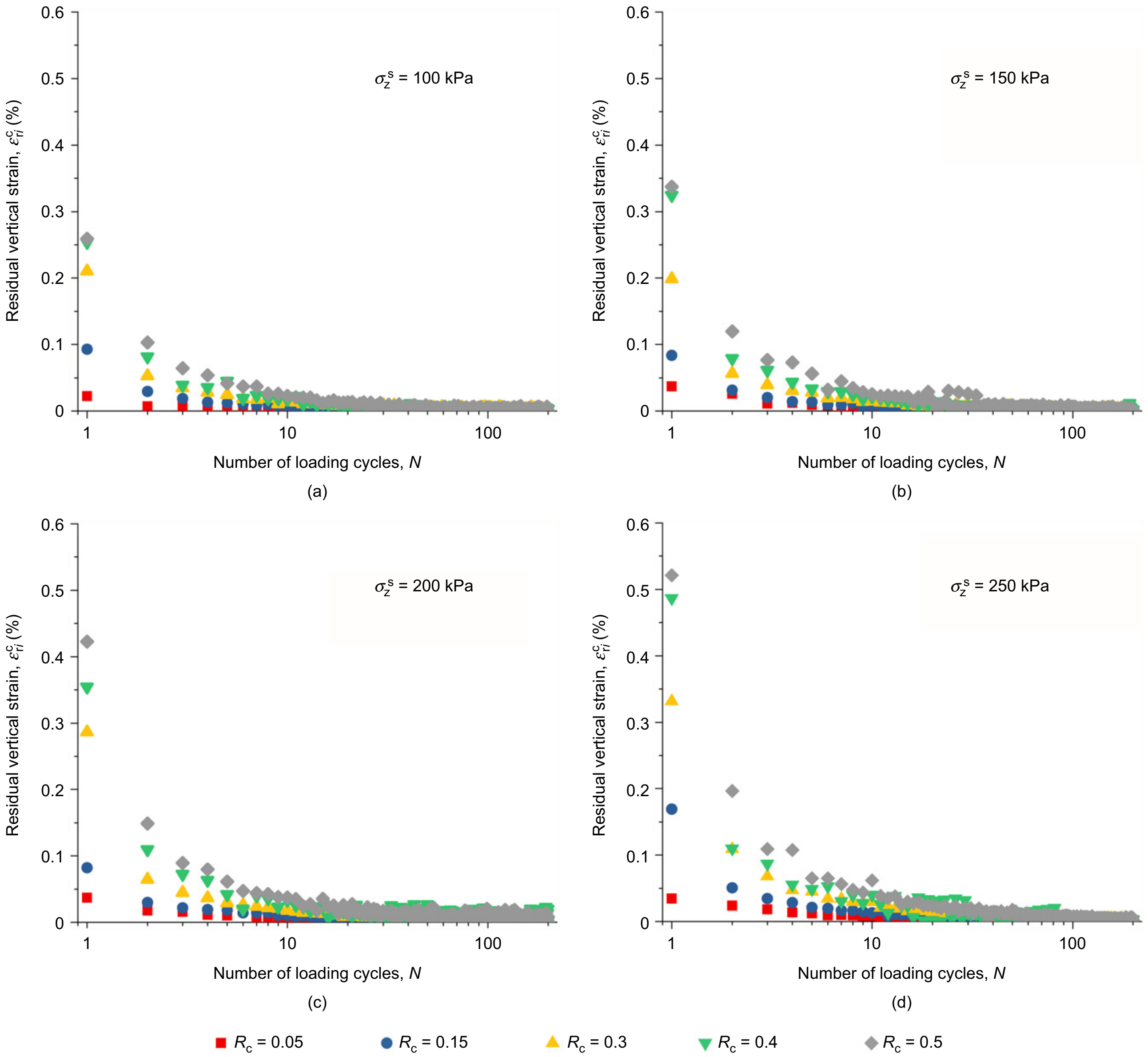

Figure 9. Residual vertical strain (ε_{ri}^c) of stacked soilbags within each loading cycle at different static vertical stresses and cyclic load ratios: (a) $\sigma_z^s = 100$ kPa; (b) $\sigma_z^s = 150$ kPa; (c) $\sigma_z^s = 200$ kPa; (d) $\sigma_z^s = 250$ kPa

Offprint provided courtesy of www.icevirtuallibrary.com
Author copy for personal use, not for distribution

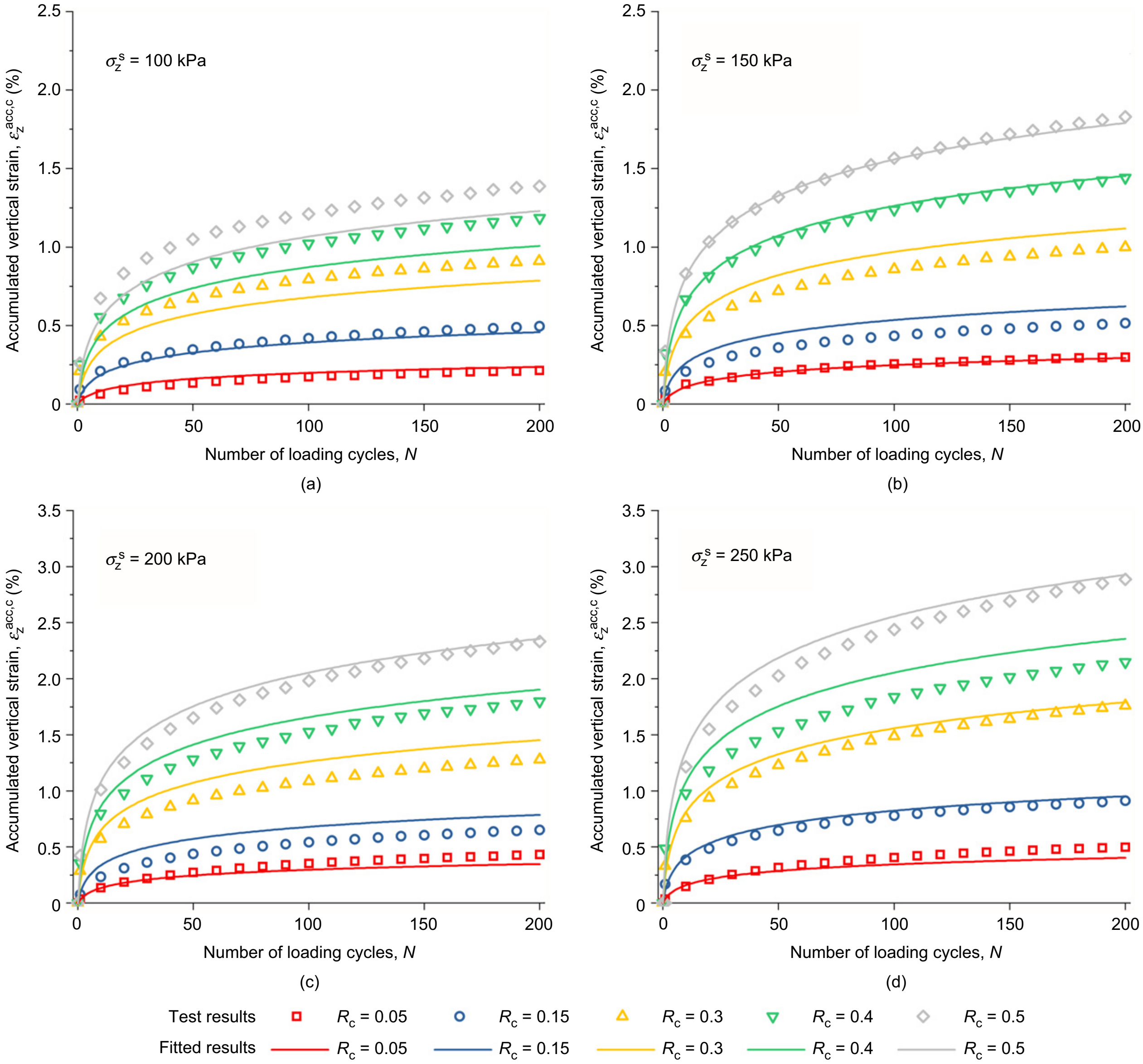

Figure 10. Evolution of accumulated vertical strain ($\varepsilon_z^{acc,c}$) of stacked soilbags with the increasing number of loading cycles (N) at different static vertical stresses and cyclic load ratios: (a) $\sigma_z^s = 100$ kPa; (b) $\sigma_z^s = 150$ kPa; (c) $\sigma_z^s = 200$ kPa; (d) $\sigma_z^s = 250$ kPa

numbers of stacked layers under monotonic loading. It shows that the vertical stress increases nonlinearly with the increasing strain during the initial loading period, indicating the gradual increase on compression modulus of stacked soilbags. With the densification of stacked soilbags under vertical compression, the stress-strain relation curve gradually becomes linear, exhibiting elastic behaviour. The vertical strains at the inflection points are approximately 8.66%, 6.55%, 5.59%, 5.02%, 4.71% and 4.43%, respectively, for 1, 2, 3, 4, 5 and 6 layers, which indicates that soilbags begin to exert a constraining effect after compaction. That is to say, before the inflection point, the tensile force has not yet been developed, and the stress of the filled soil is mainly attributed to the externally-applied vertical load. The ultimate compressive strength of the stacked soilbags is plotted against the number of stacked layers L in Figure 5b. It indicates that the ultimate compressive strength of single- and two-layered soilbags are much higher than others. This is because both the upper and the lower of the single- and two-layered soilbags are restricted by rigid steel loading plates, which has great hoop and boundary effects on soilbags. The influence of rigid steel loading plates and the ultimate compressive strength reduce as the number of stacked layers increases. The variation of the ultimate compressive strength becomes small when the number of stacked layers exceeds three. The ultimate compressive strength is nearly 0.7 MPa for six-layered soilbags, which can meet the requirement of the bearing capacity of foundations for most low-rise or middle-rise buildings (usually less than 300 kPa).

Figure 6 gives the tangent compression moduli E_{st} of stacked soilbags with different layers under monotonic loading. It indicates that the single- and two-layered soilbags have much higher E_{st} than others in accordance with the stress-strain response. The tangent compression moduli E_{st} of stacked soilbags increase continuously in the

Offprint provided courtesy of www.icevirtuallibrary.com
Author copy for personal use, not for distribution

initial loading period. They have a small sudden increase near the inflection point of the stress-strain relation curves, and then reach a peak value. After that, E_{st} reduces slightly as the vertical strain increases. The evolution of E_{st} is in good agreement with the stress-strain responses as shown in Figure 5a. At the initial stage of vertical loading, E_{st} increases significantly with the densification of stacked soilbags caused by particle rearrangement. As shown in Figure 6b, the maximum tangent compression modulus (peak value) reduces as the number of stacked layers increases and changes slightly when the number of stacked layers exceeds three. The maximum tangent compression modulus of three-layered soilbags is nearly 6.73 MPa.

The test results illustrate that the ultimate compressive strength and the tangent compression modulus of single- and two-layered soilbags are significantly influenced by the top and the bottom rigid steel loading plates, which reduce with increasing number of soilbag layers.

3.2. Cyclic loading response of stacked soilbags

3.2.1. *Overall cyclic compression behaviour*

A series of cyclic loading tests were conducted on the stacked soilbags under different static vertical stresses σ_z^s and cyclic load ratios R_c. Figure 7 gives one typical compression curve of the test, in which Figure 7a shows the evolution of the vertical strain ε_z with the loading time T and Figure 7b shows the applied vertical stress against the generated vertical strain. It can be seen that the vertical strain is mainly generated in the static loading period, and the vertical strain increases more significantly in the initial few cycles, especially in the first cycle. At the static loading stage, the stress-strain relation curve is concave upward, that is, the tangent compression modulus increases obviously. This phenomenon agrees with the results of the monotonic loading tests, as shown in Figure 5a.

Figure 8 shows the hysteresis loops of stacked soilbags under cyclic loading for different cyclic load ratios ($R_c = 0.05$, 0.15, 0.3, 0.4 and 0.5) at $\sigma_z^s = 250$ kPa. To clearly demonstrate the variation of the hysteresis loops with the increasing number of loading cycles, the hysteresis loops at $N = 2$, 10, 25, 50, 100, 150 and 200 were respectively plotted with thick curves. It can be seen that the hysteresis loops are unclosed at the bottom and have relatively large areas in initial cycles. The unclosed hysteresis loop means the development of plastic deformation. The large area of the hysteresis loop reflects the great energy dissipation of stacked soilbags under cyclic loading. With the increasing number of loading cycles, the hysteresis loop tends to close, accompanying with the decrease of the hysteresis loop area. After 100 cycles, the hysteresis loop area tends to zero and the adjacent hysteresis loops almost overlap. The narrowed and enclosed hysteresis loops indicate that the dissipated energy of stacked soilbags generated in one loading cycle decrease while the plastic deformation generated is relatively small or even zero. Actually, the seismic attenuation performance and isolation property of soilbag-isolated layer under vertical seismic motion are mainly attributed to the barrier for seismic wave passing through gaps among stacked soilbags. The studies on base isolation material under vertical seismic motion are usually focused on the bearing capacity and the stability of dynamic deformation behaviour (*e.g.* Kelly 1993; Warn *et al.* 2007). To function as a bearing structure, the soilbags-isolated layer is required to have small and stable deformation behaviour under vertical seismic motion. Therefore, the properties of the narrowed and enclosed hysteresis loops in the vertical cyclic loading period

Table 2. Constants of modified formulas fitted by test results

Fitted parameters	Value
l_1	0.03546
l_2	0.00403
l_3	0.27316
l_4	0.5014
c_1	0.45916
c_2	−0.32174
c_3	0.38579
c_4	0.19745

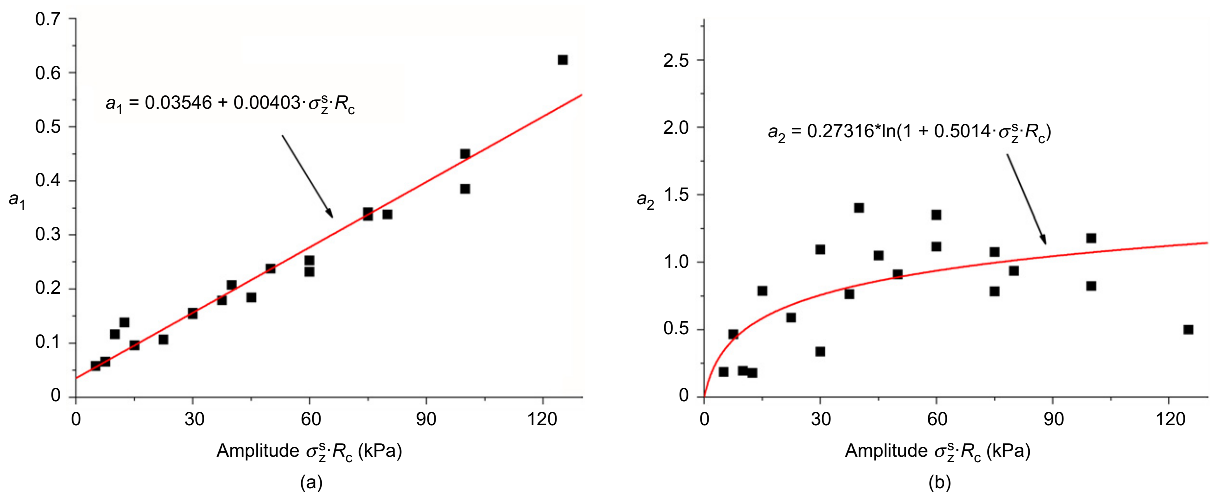

Figure 11. Parameters a_1 and a_2 calibrated with the test data: (a) $a_1 \sim (\sigma_z^s \cdot R_c)$; (b) $a_2 \sim (\sigma_z^s \cdot R_c)$

Offprint provided courtesy of www.icevirtuallibrary.com
Author copy for personal use, not for distribution

demonstrate the potential use of soilbags as a base isolation material.

3.2.2. *Accumulated vertical strain during cyclic loading period*

As shown in Figure 7, the vertical strain of the stacked soilbags comprises the development in static loading period $\varepsilon_z^{\mathrm{acc},s}$ and the other accumulation in cyclic loading period $\varepsilon_z^{\mathrm{acc},c}$. For the use of soilbags on base isolation layers, the vertical strain at static compaction mainly develops during the construction of the foundation and superstructure. The accumulated vertical strain of the stacked soilbags under cyclic loading is of importance to the base isolation layer.

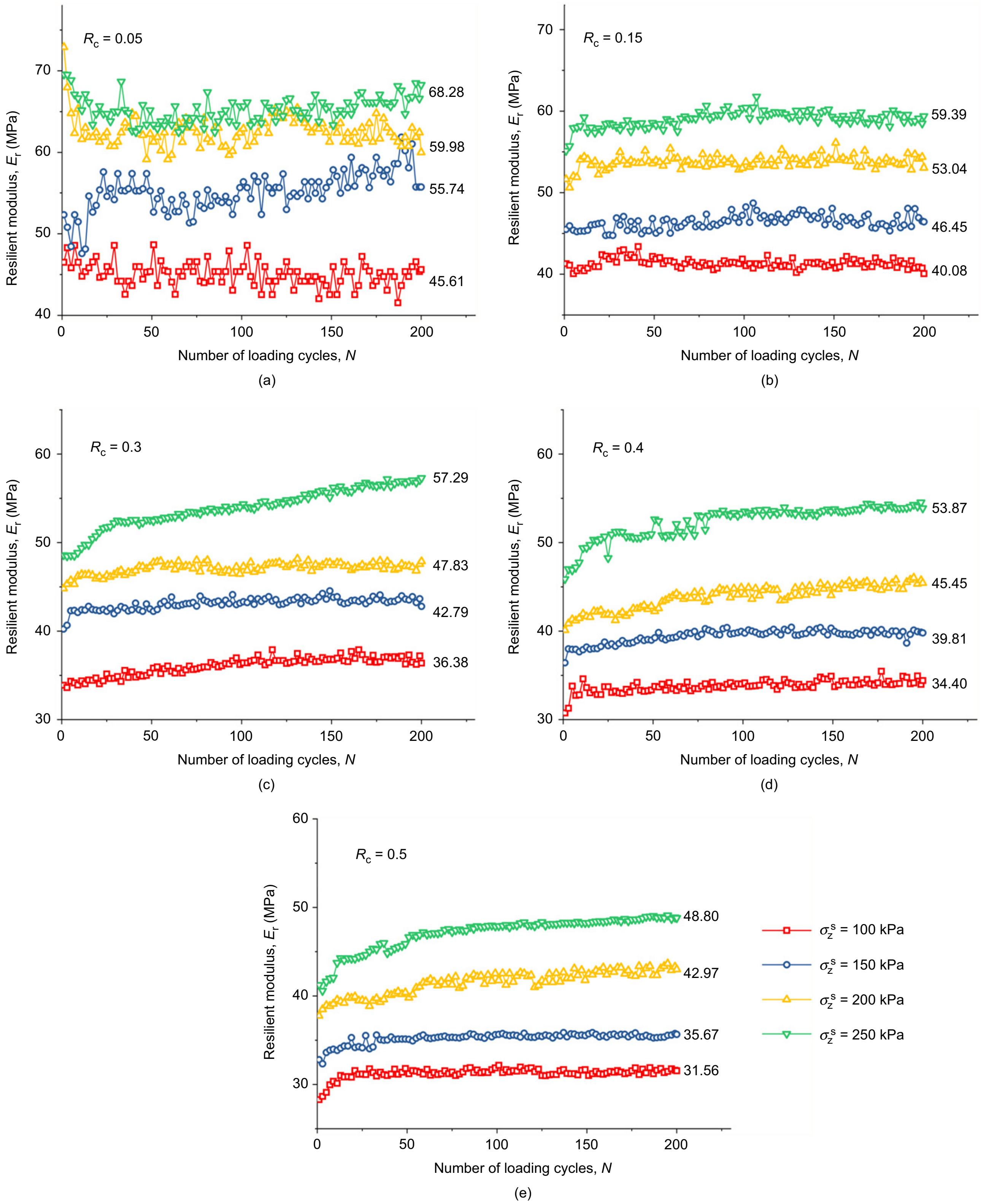

Figure 12. Resilient modulus (E_r) of stacked soilbags versus number of loading cycles: (a) $R_c = 0.05$; (b) $R_c = 0.15$; (c) $R_c = 0.3$; (d) $R_c = 0.4$; (e) $R_c = 0.5$

Offprint provided courtesy of www.icevirtuallibrary.com
Author copy for personal use, not for distribution

In this study, the residual vertical strain of the stacked soilbags within the ith loading cycle, expressed as ε_{ri}^{c}, was defined as the increment of the vertical strain at the end and the beginning of the ith loading cycle. Figure 9 shows the residual vertical strain of the stacked soilbags within each loading cycle, subjected to cyclic load ratios of $R_c = 0.05, 0.15, 0.3, 0.4$ and 0.5, under different static vertical stresses of $\sigma_z^s = 100$ kPa, 150 kPa, 200 kPa and 250 kPa. The abscissa coordinate for the number of loading cycles N was expressed in logarithmic form to clearly demonstrate the development of the residual vertical strain in the initial few loading cycles. Figure 9 illustrates that the residual vertical strain ε_{ri}^{c} reduces significantly in the initial few loading cycles and then tends to a relatively small value or even zero after several loading cycles. At the same static vertical stress σ_z^s, the residual vertical strain ε_{ri}^{c} increases with the increasing cyclic load ratio R_c. At the same R_c, the greater σ_z^s is, the larger ε_{ri}^{c} develops.

As one base isolation material, soilbags are required to deform steadily under dynamic loadings. Thus, it is necessary to investigate the accumulated vertical strain, denoted as $\varepsilon_z^{acc,c}$, of the stacked soilbags under cyclic loading, which can be obtained by accumulating the residual vertical strain ε_{ri}^{c} within each loading cycle. Figure 10 shows the evolution of the accumulated vertical strain $\varepsilon_z^{acc,c}$ of stacked soilbags with the increasing number of loading cycles at different static vertical stresses σ_z^s and cyclic load ratios R_c. It can be found that σ_z^s and R_c both positively affect the accumulated vertical strain of the stacked soilbags under cyclic loading. $\varepsilon_z^{acc,c}$ increases nonlinearly under the application of cyclic loading, accompanied with a reducing ε_{ri}^{c}, and subsequently reaches a relatively stable state where the vertical strain is primarily elastic (Werkmeister *et al.* 2004). This characteristic may be defined as 'plastic shakedown' (Werkmeister *et al.* 2001; Moghaddas Tafreshi *et al.* 2019) where the stacked soilbags achieve a long-term

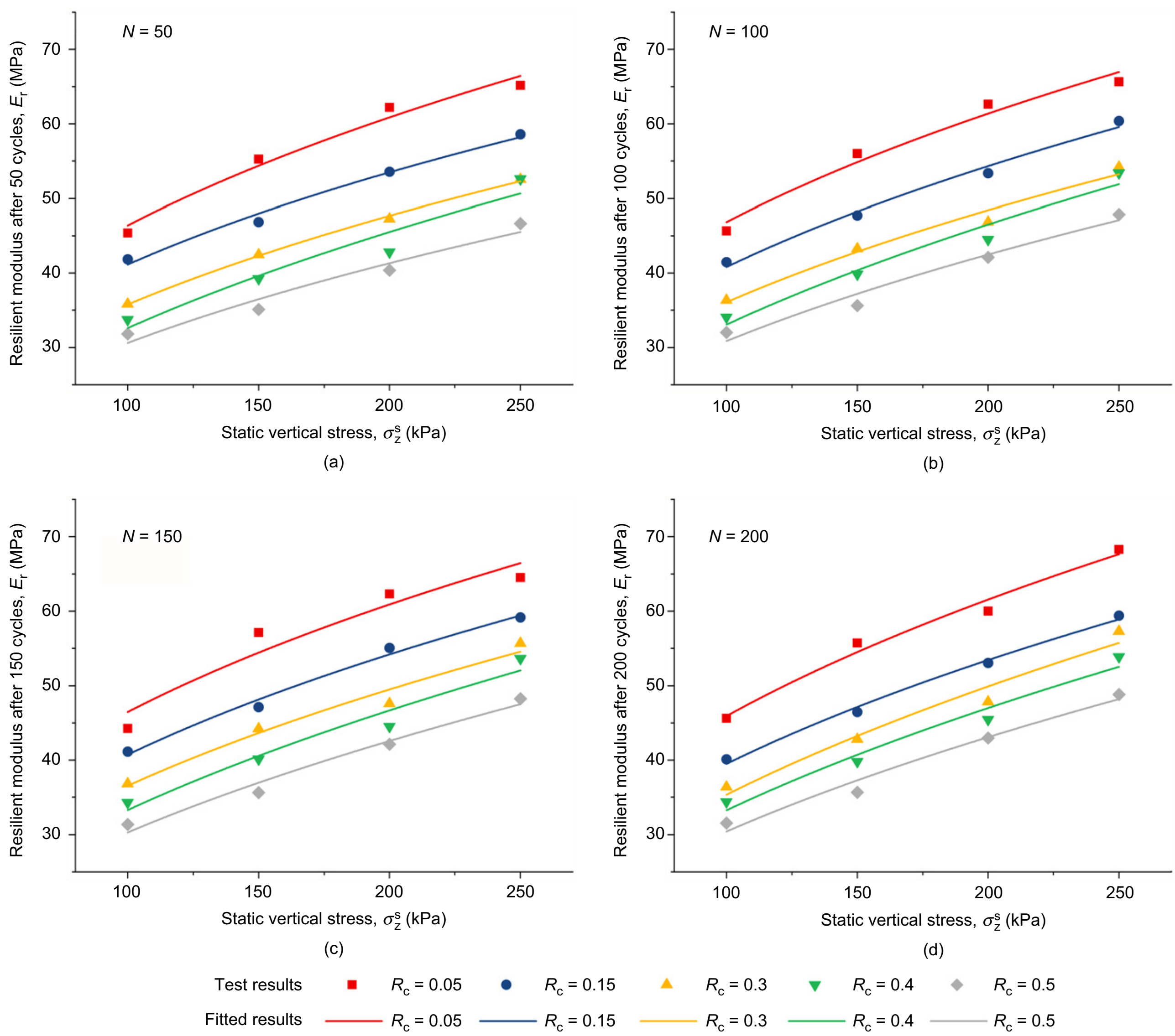

Figure 13. Resilient moduli (E_r) of stacked soilbags after several loading cycles versus static vertical stress (σ_z^s) for different cyclic load ratios (R_c): (a) $N = 50$; (b) $N = 100$; (c) $N = 150$; (d) $N = 200$

Offprint provided courtesy of www.icevirtuallibrary.com
Author copy for personal use, not for distribution

and steady-state response. The plastic shakedown of the accumulated vertical strain of the stacked soilbags under cyclic loading suggests that soilbags used in the base isolation of buildings are feasible.

For non-cohesive soils under cyclic loading, Karg *et al.* (2010) put forward an empirical formula to describe such a shape of compaction curve that the vertical strain increases rapidly in the initial few loading cycles, gradually reaching a relatively stable state. They characterized the accumulated vertical strain during the cyclic loading period as the sum of an initial logarithmic growth in the initial few loading cycles and a linear growth after a certain number of loading cycles, expressed as:

$$\varepsilon_z^{acc,c} = a_1 \ln(1 + a_2 N) + a_3 N \tag{4}$$

where a_1, a_2 and a_3 are the fitting parameters, and N is the number of loading cycles.

In this study, a similar fitted formula for the accumulated vertical strain $\varepsilon_z^{\mathrm{acc},c}$ of the stacked soilbags under cyclic loading was proposed:

$$\varepsilon_z^{acc,c} = a_1 \ln(1 + a_2 N) \tag{5}$$

where the term $(a_3 N)$ in Equation (4) reflecting the linear growth after a certain number of loading cycles was omitted in consideration of the small residual vertical strain $\varepsilon_{\mathrm{r}i}^{\mathrm{c}}$ after several loading cycles (see Figure 9). The parameters a_1 and a_2 were proved to be correlated to the cyclic loading amplitude $(\sigma_z^s \cdot R_c)$ after regression on the test results, respectively expressed as:

$$a_1 = l_1 + l_2 \sigma_{\mathrm{z}}^s R_c \tag{6}$$

$$a_2 = l_3 \ln\left(1 + l_4 \sigma_{\mathrm{z}}^s R_c\right) \tag{7}$$

where l_1, l_2, l_3 and l_4 are the fitted constants, as listed in Table 2. The fitted parameters a_1 and a_2 based on the test results were shown in Figure 11. In spite of some scattered test points, the parameters a_1 and a_2 can be respectively fitted with a linear line and a logarithmic curve, as shown in Figure 11.

The fitted curves by using Equations (5)–(7) for different static vertical stresses and cyclic load ratios are also presented in Figure 10. The modified formula for $\varepsilon_{\mathrm{z}}^{\mathrm{acc,c}}$ can effectively describe the process of the vertical strain accumulation and the characteristic of stabilization of soilbags under cyclic loading at different cyclic loading amplitudes $(\sigma_z^s \cdot R_c)$. A good agreement with the test data can be observed, especially under relatively high-stress conditions.

3.2.3. *Resilient modulus*

The resilient modulus is a significant parameter for the design of the base isolation systems. Therefore, it is necessary to investigate the resilient modulus of stacked soilbags under cyclic loading and establish models or empirical formulas for the resilient modulus. Figure 12 shows the variation of the resilient modulus E_{r} of the stacked soilbags, calculated by Equation (3), with the increasing number of loading cycles at different static vertical stresses and cyclic load ratios. As shown in Figure 12a, at the low cyclic load ratio $R_{\mathrm{c}} = 0.05$, the resilient moduli fluctuate slightly with the increasing number of loading cycles, which might result from the measurement precision. On the whole, the resilient moduli of the stacked soilbags under different cyclic loading amplitudes change slightly during the cyclic loading period in accordance with the slopes of the hysteresis loops in Figure 8. It is evident here that the resilient modulus E_{r} increases significantly with the increasing static vertical stress σ_z^s at the same cyclic load ratio R_{c}, whereas E_{r} is negatively correlated with the cyclic load ratio R_{c} at the same σ_z^s. Figure 13 presents the variation of the resilient modulus with the static vertical stress at different cyclic load ratios and loading cycle numbers. The test results demonstrate that the resilient modulus of the stacked soilbags depends on the static vertical stress and the cyclic load ratio, and is influenced slightly by the number of loading cycles.

In previous studies, some empirical formulas for the resilient modulus of non-cohesive soils under cyclic loading have been proposed (Lekarp *et al.* 2000; Parreira and Gonçalves 2000; Salour and Erlingsson 2015; Pereira *et al.* 2017). In this study, referred to the empirical formula proposed by Hicks (1970), the following empirical formula was suggested to calculate the resilient modulus of soilbags.

$$E_{\mathrm{r}} = n_1 p_a \left(\frac{\sigma_z^s}{p_a}\right)^{n_2} \tag{8}$$

where n_1 and n_2 are parameters fitted by the test results, and p_{a} is the atmospheric pressure (100 kPa). The curves in Figure 13 are fitted by Equation (8), and the fitted parameters n_1 and n_2 at different cyclic load ratios R_{c} are

Table 3. Fitted parameters of modified formula for resilient modulus

Cyclic load ratio R_{c}	Number of loading cycles N	Fitted parameters		
		n_1	n_2	R^2
$R_{\mathrm{c}} = 0.05$	$N = 50$	0.46378	0.39211	0.96598
	$N = 100$	0.46828	0.39012	0.96184
	$N = 150$	0.46459	0.3903	0.89192
	$N = 200$	0.45916	0.42276	0.97467
$R_{\mathrm{c}} = 0.15$	$N = 50$	0.4114	0.37855	0.9825
	$N = 100$	0.4081	0.41248	0.98277
	$N = 150$	0.40735	0.41168	0.98499
	$N = 200$	0.39495	0.43593	0.99125
$R_{\mathrm{c}} = 0.3$	$N = 50$	0.35772	0.41425	0.9974
	$N = 100$	0.36078	0.42453	0.96751
	$N = 150$	0.36555	0.43689	0.95688
	$N = 200$	0.35359	0.49666	0.94937
$R_{\mathrm{c}} = 0.4$	$N = 50$	0.32603	0.48081	0.8999
	$N = 100$	0.33073	0.49162	0.94465
	$N = 150$	0.33292	0.4873	0.9356
	$N = 200$	0.3326	0.49853	0.95415
$R_{\mathrm{c}} = 0.5$	$N = 50$	0.30606	0.43291	0.93608
	$N = 100$	0.30861	0.46117	0.95462
	$N = 150$	0.30291	0.4909	0.96704
	$N = 200$	0.30417	0.50204	0.96325

Offprint provided courtesy of www.icevirtuallibrary.com
Author copy for personal use, not for distribution

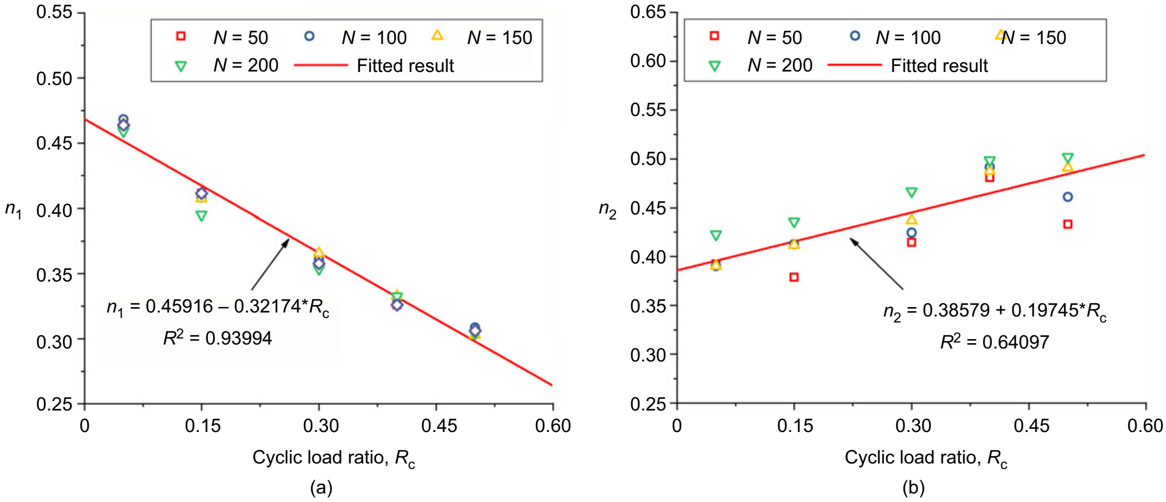

Figure 14. Determination of two parameters (n_1 and n_2) in Equation (8) versus cyclic load ratio (R_c): (a) $n_1 \sim R_c$; (b) $n_2 \sim R_c$

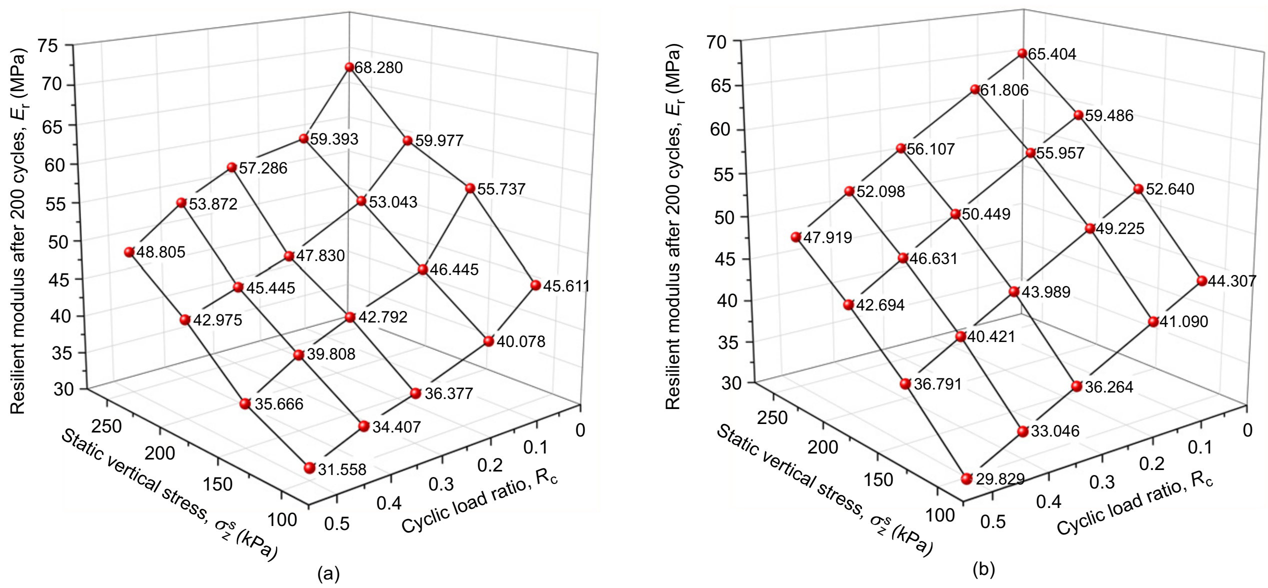

Figure 15. Resilient modulus (E_r) of stacked soilbags after 200 cycles at different static vertical stresses (σ_z^s) and cyclic load ratios (R_c): (a) test results; (b) calculated results

given in Table 3. Furthermore, the parameters n_1 and n_2 are proved to be correlated with R_c as presented in Figure 14. It shows that the parameter n_1 almost increases linearly with R_c and conversely for the parameter n_2. Thus, Equation (8) can be rewritten as:

$$E_r = (c_1 + c_2 R_c) \cdot p_a \cdot \left(\frac{\sigma_z^s}{p_a}\right)^{(c_3 + c_4 R_c)} \quad (9)$$

where c_1, c_2, c_3 and c_4 are the constants fitted by the test results, as listed in Table 2.

The test results and calculated results of the resilient modulus of the stacked soilbags are plotted in Figure 15. It is evident here that the calculated results presented in Figure 15b agree with the test results in Figure 15a. This means that the modified formula for E_r can reflect the influence of the static vertical stress σ_z^s and the cyclic load ratio R_c on the variation of resilient modulus.

4. CONCLUSIONS

In this study, a series of laboratory unconfined compression tests including the monotonic loading tests and the cyclic loading tests have been carried out on stacked soilbags. The influences of the static vertical stress σ_z^s and the cyclic load ratio R_c as well as the number of loading cycles N on the dynamic deformation behaviour of stacked soilbags were investigated. Empirical formulas were proposed to respectively describe the variations of the accumulated vertical strains and the resilient moduli of stacked soilbags under different vertical stresses and cyclic load ratios. The main conclusions are obtained as follows:

(*a*) The ultimate compressive strength of single- or two-layered soilbags is influenced significantly by top and bottom rigid steel bearing plates in the monotonic loading tests owing to the hoop effect and

Offprint provided courtesy of www.icevirtuallibrary.com
Author copy for personal use, not for distribution

the boundary effect. When the number of stacked layers exceeds three, the ultimate compressive strength tends to a relatively stable value of around 0.7 MPa, which can meet the requirement of the bearing capacity of foundations for most low-rise or middle-rise buildings (usually less than 300 kPa). Meanwhile, the tangent compression modulus has a relatively stable value of around 6.73 MPa.

(*b*) In the cyclic loading tests, the hysteresis loops are unclosed at the bottom and have relatively large areas in the initial loading cycles. With the increasing number of loading cycles, the hysteresis loop tends to close, accompanied by the decrease of the hysteresis loop area. The accumulated vertical strain $\varepsilon_z^{\mathrm{acc,c}}$ increases nonlinearly under cyclic loading, accompanied with a reducing residual vertical strain $\varepsilon_{\mathrm{r}i}^{\mathrm{c}}$, and subsequently reaches a relatively stable state where the vertical strain is primarily elastic. This dynamic deformation behaviour can be described with an empirical formula (Equation (5)) which is positively correlated with the static vertical stress, the cyclic load ratio and the number of loading cycles.

(*c*) During the cyclic loading period, the resilient moduli of the stacked soilbags under different cyclic loading amplitudes change slightly; however, E_{r} increases significantly with the increasing static vertical stress σ_z^s at the same cyclic load ratio R_{c}, whereas E_{r} is negatively correlated with the cyclic load ratio R_{c} at the same σ_z^s. The variation of the resilient modulus can be described with Equation (9), which is correlated with the static vertical stress σ_z^s and the cyclic load ratio R_{c}.

The outcomes of this study demonstrate the potential use of soilbags as a base isolation material since soilbags have large bearing capacity and stable deformation behaviour under cyclic loadings. In addition, as a base isolation material, the dynamic deformation behaviour and the elastic recoverability of soilbags under horizontal dynamic loads should also be investigated in future studies.

ACKNOWLEDGEMENTS

The work presented in this paper was supported by the National Key R&D Program of China (Grant No. 2017YFE0128900), the National Natural Science Foundation of China (Grant No. 52109123) and China Postdoctoral Science Foundation (Grant No. 2021M690878). These financial supports are gratefully acknowledged.

NOTATION

Basic SI units are given in parentheses.

A_0	initial area of stacked soilbags (m^2)
a_1, a_2, a_3	parameters of Equation (4) for accumulated vertical strain (dimensionless)
c_1, c_2, c_3, c_4	constants of Equation (9) for resilient modulus (dimensionless)
E_{r}	resilient modulus of stacked soilbags in one loading cycle (Pa)
E_{st}	tangent compression modulus of soilbags (Pa)
h_0	initial height of stacked soilbags (m)
L	number of stacked layers (dimensionless)
l_1, l_2, l_3, l_4	constants of Equation (5) for accumulated vertical strain (dimensionless)
N	number of loading cycles (dimensionless)
n_1, n_2	parameters of Equation (8) for resilient modulus (dimensionless)
P	vertical load of stacked soilbags (N)
P_{cyc}	cyclic load (N)
P_{stat}	static load (N)
p_{a}	atmospheric pressure (Pa)
R_{c}	cyclic load ratio (dimensionless)
T	time (s)
$\Delta\varepsilon_{\mathrm{z}}$	increment of vertical strains (dimensionless)
$\Delta\varepsilon_z^e$	elastic vertical strain in one loading cycle (dimensionless)
$\Delta\varepsilon_z^p$	plastic vertical strain in one loading cycle (dimensionless)
$\Delta\sigma_z$	increment of vertical stresses (Pa)
δ	vertical displacement of stacked soilbags (m)
$\varepsilon_{\mathrm{r}i}^{\mathrm{c}}$	vertical residual strain in *i*th loading cycle (dimensionless)
ε_{z}	vertical strain of stacked soilbags (dimensionless)
$\varepsilon_z^{\mathrm{acc},c}$	accumulated vertical strain in the cyclic loading period (dimensionless)
$\varepsilon_z^{\mathrm{acc},s}$	accumulated vertical strain in the static loading period (dimensionless)
θ	inclination angle measured by connecting the two endpoints of the unloading curve in one loading cycle (rad)
σ_z	vertical stress of stacked soilbags (Pa)
σ_z^s	static vertical stress (Pa)

REFERENCES

Ahmad, S., Ghani, F. & Adil, M. R. (2009). Seismic friction base isolation performance using demolished waste in masonry housing. *Construction and Building Materials*, **23**, No. 1, 146–152.

Ansari, Y., Merifield, R., Yamamoto, H. & Sheng, D. C. (2011). Numerical analysis of soilbags under compression and cyclic shear. *Computers and Geotechnics*, **38**, No. 5, 659–668.

Cheng, H. Y., Yamamoto, H. & Thoeni, K. (2016). Numerical study on stress states and fabric anisotropies in soilbags using the DEM. *Computers and Geotechnics*, **76**, 170–183.

Fenz, D. M. & Constantinou, M. C. (2006). Behaviour of the double concave friction pendulum bearing. *Earthquake Engineering & Structural Dynamics*, **35**, No. 11, 1403–1424.

Hicks, R. G. (1970). *Factors Influencing the Resilient Properties of Granular Materials*. PhD, University of California, Berkeley, CA, USA.

Offprint provided courtesy of www.icevirtuallibrary.com
Author copy for personal use, not for distribution

Karg, C., François, S., Haegeman, W. & Degrande, G. (2010). Elasto-plastic long-term behavior of granular soils: modelling and experimental validation. *Soil Dynamics and Earthquake Engineering,* **30**, No. 8, 635–646.

Kelly, J. M. (1993). *Earthquake-resistant Design with Rubber*. Springer, London, UK.

Lekarp, F., Isacsson, U. & Dawson, A. (2000). State of the art. I: Resilient response of unbound aggregates. *Journal of Transportation Engineering,* **126**, No. 1, 66–75.

Liu, S. H. (2017). *Principle and Application of Soilbags*. Science Press, Beijing, China (in Chinese).

Liu, S. H. & Matsuoka, H. (2007). A new earth reinforcement method by soilbags. *Rock and Soil Mechanics*, **28**, No. 8, 1665–1670 (in Chinese).

Liu, S. H., Wang, Y. Q., Hu, X. P. & Li, Y. J. (2010). *Soilbag-isolated foundation and construction method and application*. Chinese Patent No. 201010239164 (in Chinese).

Liu, S. H., Gao, J. J., Wang, Y. Q. & Weng, L. P. (2014). Experimental study on vibration reduction by using soilbags. *Geotextiles and Geomembranes*, **42**, No. 1, 52–62.

Liu, S. H., Lu, Y., Weng, L. P. & Bai, F. Q. (2015). Field study of treatment for expansive soil/rock channel slope with soilbags. *Geotextiles and Geomembranes*, **43**, No. 4, 283–292.

Liu, S. H., Jia, F., Chen, X. L. & Li, L. J. (2020). Experimental study on seismic response of soilbags-built retaining wall. *Geotextiles and Geomembranes*, **48**, No. 5, 603–613.

Liu, S. H., Liao, J., Bong, T. T. & Fan, K. W. (2021). Repeated loading of soilbag-reinforced road subgrade. *Geosynthetics International*, **28**, No. 2, 113–124.

Lohani, T. N., Matsushima, K., Aqil, U., Mohri, Y. & Tatsuoka, F. (2006). Evaluating the strength and deformation characteristics of a soil bag pile from full-scale laboratory tests. *Geosynthetics International,* **13**, No. 6, 246–264.

Matsuoka, H. & Liu, S. H. (1999). Bearing capacity improvement by wrapping a part of foundation. *Doboku Gakkai Ronbunshu,* **617**, 235–249 (in Japanese).

Matsuoka, H. & Liu, S. H. (2003). New earth reinforcement method by soilbags ('Donow'). *Soils and Foundations*, **43**, No. 6, 173–188.

Moghaddas Tafreshi, S. N., Rahimi, M., Dawson, A. & Leshchinsky, B. (2019). Cyclic and post-cycling anchor response in geocell-reinforced sand. *Canadian Geotechnical Journal*, **56**, No. 11, 1700–1718.

MOHURD (2011). *Code for Design of Building Foundation*. China Architecture and Building Press, Beijing, China (in Chinese).

Mosqueda, G., Whittaker, A. S. & Fenves, G. L. (2004). Characterization and modeling of friction pendulum bearings subjected to multiple components of excitation. *Journal of Structural Engineering*, **130**, No. 3, 433–442.

Nanda, R. P., Agarwal, P. & Shrikhande, M. (2012). Suitable friction sliding materials for base isolation of masonry buildings. *Shock and Vibration*, **19**, No. 6, 1327–1339.

Parreira, A. B. & Gonçalves, R. F. (2000). The influence of moisture content and soil suction on the resilient modulus of a lateritic subgrade soil. In *Proceedings of GeoEng International Conference on Geotechnical and Geological Engineering*, Melbourne, Australia.

Pereira, C., Nazarian, S. & Correia, A. G. (2017). Extracting damping information from resilient modulus tests. *Journal of Materials in Civil Engineering*, **29**, No. 12, 04017233.

Robinson, W. H. (1982). Lead-rubber hysteretic bearings suitable for protecting structures during earthquakes. *Earthquake Engineering & Structural Dynamics*, **10**, No. 4, 593–604.

Salour, F. & Erlingsson, S. (2015). Resilient modulus modelling of unsaturated subgrade soils: laboratory investigation of silty sand subgrade. *Road Materials and Pavement Design,* **16**, No. 3, 553–568.

Sheng, T., Bian, X. C., Liu, G. B., Xiao, C., Chen, Y. & Li, Y. (2020). Experimental study on the sandbag isolator of buildings for subway-induced vertical vibration and secondary air-borne noise. *Geotextiles and Geomembranes*, **48**, No. 4, 504–515.

Tantono, S. F. & Bauer, E. (2008). Numerical simulation of a soilbag under vertical compression. In *Proceedings of the 12th International Conference of International Association for Computer Methods and Advances in Geomechanics (IACMAG)*, Goa, India, pp. 433–439.

Tsang, H. H. (2008). Seismic isolation by rubber–soil mixtures for developing countries. *Earthquake Engineering & Structural Dynamics*, **37**, No. 2, 283–303.

Wang, Y. Q., Li, X., Liu, K. & Liu, G. (2019). Experiments and DEM analysis on vibration reduction of soilbags. *Geosynthetics International*, **26**, No. 5, 551–562.

Warn, G. P., Whittaker, A. S. & Constantinou, M. C. (2007). Vertical stiffness of elastomeric and lead–rubber seismic isolation bearings. *Journal of Structural Engineering*, **133**, No. 9, 1227–1236.

Werkmeister, S., Dawson, A. R. & Wellner, F. (2001). Permanent deformation behavior of granular materials and the shakedown concept. *Transportation Research Record*, **1757**, 75–81.

Werkmeister, S., Dawson, A. R. & Wellner, F. (2004). Pavement design model for unbound granular materials. *Journal of Transportation Engineering*, **130**, No. 5, 665–674.

Yamamoto, H., Matsuoka, H., Simao, R., Hasebe, T. & Hattori, M. (2003). Cyclic shear property and damping ratio of soilbag assembly. In *Proceedings of the 38th Japan National Conference on Geotechnical Engineering*, Akita, Japan, pp. 757–758.

Yao, F., Shang, S. P. & Liu, K. (2014). Shake table tests of a new steel–asphalt composite layer system for the seismic base isolation of housing units. *Soil Dynamics and Earthquake Engineering*, **59**, 1–7.

The Editor welcomes discussion on all papers published in Geosynthetics International. Please email your contribution to discussion@geosynthetics-international.com

Offprint provided courtesy of www.icevirtuallibrary.com
Author copy for personal use, not for distribution